Mechanistic, Mutational, and Structural Evaluation of a *Taxus* Phenylalanine Aminomutase

Lei Feng,[†,§] Udayanga Wanninayake,[†,§] Susan Strom, James Geiger,*[†] and Kevin D. Walker*[†,‡]

[†]Department of Chemistry, Michigan State University, East Lansing, Michigan 48824, United States

[‡]Department of Biochemistry and Molecular Biology, Michigan State University, East Lansing, Michigan 48824, United States

Ⓢ *Supporting Information*

ABSTRACT: The structure of a phenylalanine aminomutase (*Tc*PAM) from *Taxus canadensis* has been determined at 2.4 Å resolution. The active site of the *Tc*PAM contains the signature 4-methylidene-1*H*-imidazol-5(4*H*)-one prosthesis, observed in all catalysts of the class I lyase-like family. This catalyst isomerizes (*S*)-α-phenylalanine to the (*R*)-β-isomer by exchange of the NH_2/H pair. The stereochemistry of the *Tc*PAM reaction product is opposite of the (*S*)-β-tyrosine made by the mechanistically related tyrosine aminomutase (*Sg*TAM) from *Streptomyces globisporus*.

Since *Tc*PAM and *Sg*TAM share similar tertiary- and quaternary-structures and have several highly conserved aliphatic residues positioned analogously in their active sites for substrate recognition, the divergent product stereochemistries of these catalysts likely cannot be explained by differences in active site architecture. The active site of the *Tc*PAM structure also is in complex with (E)-cinnamate; the latter functions as both a substrate and an intermediate. To account for the distinct (3*R*)-β-amino acid stereochemistry catalyzed by *Tc*PAM, the cinnamate skeleton must rotate the C_1-C_α and $C_{ipso}-C_\beta$ bonds 180° in the active site prior to exchange and rebinding of the NH_2/H pair to the cinnamate, an event that is not required for the corresponding acrylate intermediate in the *Sg*TAM reaction. Moreover, the aromatic ring of the intermediate makes only one direct hydrophobic interaction with Leu-104. A L104A mutant of *Tc*PAM demonstrated an ~1.5-fold increase in k_{cat} and a decrease in K_M values for sterically demanding 3′-methyl-α-phenylalanine and styryl-α-alanine substrates, compared to the kinetic parameters for *Tc*PAM. These parameters did not change significantly for the mutant with 4′-methyl-α-phenylalanine compared to those for *Tc*PAM.
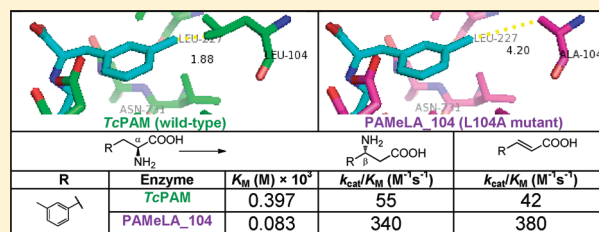
Tyrosine aminomutases from *Streptomyces globisporus* (*Sg*TAM),[1] *Chondromyces crocatus*, and *Myxococcus fulvus*,[2] and the phenylalanine aminomutase from *Taxus canadensis* (*Tc*PAM)[3] belong to the 5-methylideneimidazol-4-one (MIO) subcategory of isomerases. These isomerases show high sequence homology to a family of MIO-dependent phenylalanine, tyrosine, and histidine ammonia lyases (PAL, TAL, and HAL, respectively) whose reaction mechanism aborts after the α-NH_2/β-H-elimination from the substrate to liberate an aryl acrylate product.[4,5] On the basis of a compendium of supporting structural data, the MIO purportedly acts as an electrophile in the aminomutase active site to alkylate the substrate via direct electrophilic activation of the amino group[6] (Figure 1). This step is proposed to facilitate the elimination of the amino group, followed by enzyme-catalyzed exchange and Michael-type rebound of the labile α-NH_2/H pair to the phenylpropenoid to produce the β-amino acid (Figure 1). Residual ammonia lyase activity of the *Tc*PAM enzyme produces *trans*-cinnamic acid as a minor product compared to the β-amino acid product during steady-state catalysis;[3] the *Sg*TAM enzyme shows similar chemistry, producing *trans*-coumarate and β-tyrosine.[7] This suggests that the lyases and aminomutases follow analogous mechanistic courses and that *trans*-stereoisomers of cinnamate and coumarate

represent intermediates on the reaction pathway of the phenylalanine and tyrosine aminomutases, respectively. However, *Sg*TAM produces predominantly the corresponding (*S*)-β-tyrosine with stereochemistry opposite to that of the product made by *Tc*PAM.

The mode of β-H and NH_2 exchange was evaluated for the native *Taxus* PAM, in an early study where the bark of *Taxus brevifolia* plants was used to obtain an aqueous extract that contained a crude mixture of enzymes.[8] Likely present in the milieu were ammonia lyases, now known to be operationally similar to MIO-dependent aminomutases,[9] and other soluble enzymes involved in cinnamate metabolism (e.g., CoA ligases or hydroxylases). Cinnamate was not imagined, at the time, to participate in the reaction (KDW). To assess if the native *Taxus* PAM reaction was inter- or intramolecular, a 1:1 mixture of [ring-$^2H_5$, ^{15}N]- and unlabeled-phenylalanine was incubated with the native PAM, and gas chromatography−mass spectrometry analysis of biosynthetically derived β-phenylalanine isotopomers showed fragment ions consistent with an *intra*molecular
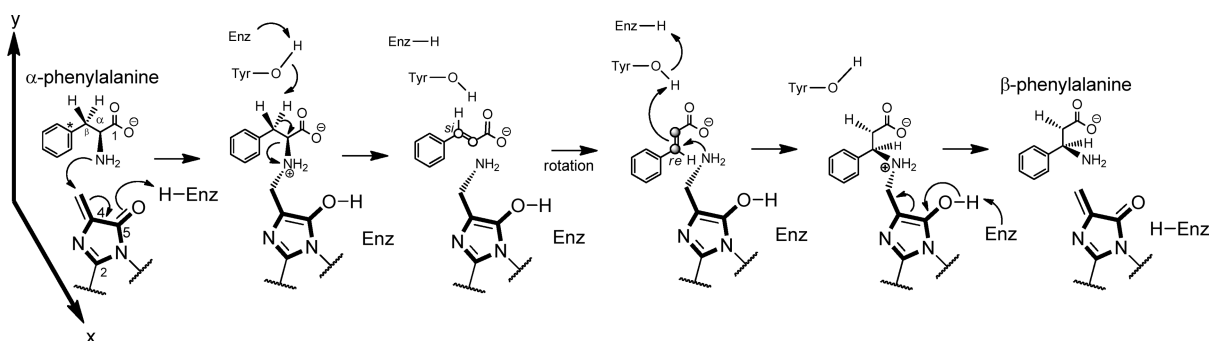
Figure 1. An MIO-dependent mechanism for TcPAM catalysis. A proposed mechanism that begins with attack on the MIO by the amine at C_α of the substrate, followed by a concerted elimination pathway to a cinnamate intermediate. Interchange of the amino group and the hydrogen and Michael-type rebound produces the β-amino acid. The step designated "rotation" signifies a rotation of the acrylate intermediate about the C_1–C_α and C_β–C_{ipso} bonds. The open circles (O) and the filled circles (●) on the cinnamate molecule are used to distinguish the si- and re-faces of the double bond, respectively, using C_β as the reference.

mechanism.[8] While this early study elucidated the mode of the NH_2-group transfer, the influence of cinnamate and other cinnamate modifying enzymes on the NH_2-transfer process was not considered.

Therefore, in this study, the intramolecular mode of NH_2-transfer was corroborated by incubating purified, recombinant TcPAM with a mixture of [ring, β-C-$^2H_6$]cinnamate and [^{15}N]-phenylalanine. This confirmatory study was important since a purified, recombinantly expressed $Taxus$ PAM was recently shown to catalyze the formation of β-phenylalanine from cinnamate and ammonia cosubstrates.[10] Also described herein is the X-ray crystal structure of a recombinant phenylalanine aminomutase–cinnamate complex at 2.4 Å resolution. This is the first structure reported on an aminomutase of plant origin and is one of two enzymes (the other is taxadiene synthase[11]) on the Taxol biosynthetic pathway whose structures have been solved. The intramolecular mechanism of the reaction in conjunction with the X-ray crystal structure answered a central question regarding how TcPAM catalyzes a different stereoisomer of its β-amino acid product compared to that of the structurally similar SgTAM.[12] Herein, evaluation of the TcPAM-cinnamate substrate/intermediate complex enabled us to posit a reaction sequence that is consistent with the stereospecificity of TcPAM catalysis and with a mode that retains the configuration at the migration termini. In addition, The TcPAM structure along with modeled-in substrates also shows that the 3'-carbon of the aromatic ring of the bound cinnamate intermediate/substrate is proximate to and makes a direct hydrophobic interaction with Leu-104. This residue and several other distal hydrophobic interactions between the aromatic ring of cinnamate and Leu-179, Leu-227, and Val-230 likely contribute to substrate binding and to defining the topology of the active site. This document describes a rational point mutation that exchanges Leu-104 for a sterically smaller Ala residue that yielded a mutant TcPAM with increased catalytic efficiencies for nonnatural arylalanines.

■ MATERIALS AND METHODS

(R)-β-Amino acids were commercially available from PepTech Corporation (Burlington, MA), except for styryl-(R)-β-alanine, which was synthesized by modification of a described procedure.[13] 5-Phenyl-($2E,4E$)-pentadienoic acid ((E,E)-styrylacrylate) was

purchased from Alfa Aesar (Ward Hill, MA). (E)-[ring, β-C-$^2H_6$]Cinnamic acid and (E)-2'methylcinnamic acid were obtained from Sigma-Aldrich (St. Louis, MO), and [^{15}N]phenylalanine was obtained from Cambridge Isotope Laboratories (Andover, MA).

Construction of Site-Directed Mutants of PAM. TcPAM point mutants were generated using the QuikChange II site-directed mutagenesis kit (Stratagene, La Jolla, CA) and Turbo Pfu polymerase (Stratagene, La Jolla, CA) along with the respective oligonucleotide primers: Y80F-For-(5'-AGACGGT GCTGATATCT**TT**GGCGTTACCACGGGTTTCGG-3') and L104A-For-(5'-GCAGGAGAGC**GCC**ATCCGCTGTC-3'). The corresponding reverse-complement primer was paired with the respective forward primer. The mutation is highlighted in bold and underlined. The pET28a expression vector DNA containing wild-type TcPAM was used as a template, and the mutation in the TcPAM gene was confirmed by DNA sequencing.

Expression and Purification of N-Terminal His-Tagged PAM. Codon-optimized wild-type[14] or a mutant TcPAM derived from the optimized clone was overexpressed in *Escherichia coli* BL21(DE3) cells. The cells (six 1-L cultures) were grown in Luria–Bertani medium supplemented with kanamycin (50 μg/mL), induced for expression with isopropyl-β-D-thiogalactopyranoside (100 μM) at 16 °C, and, after 16 h, were harvested by centrifugation (4,000g for 20 min). To the cell pellet was added 100 mL of resuspension buffer (50 mM sodium phosphate containing 10 mM imidazole, 5% (v/v) glycerol, and 300 mM NaCl, pH 8.5), the suspension was lysed by sonication, and the cellular debris and light membranes were removed by centrifugation at 9,700g (45 min) then at 102,000g (1 h), respectively. The resultant crude aminomutase in the soluble fraction was purified by nickel-nitrilotriacetic acid affinity chromatography according to the protocol described by the manufacturer (Qiagen, Valencia, CA); TcPAM was eluted in 250 mM imidazole (3 mL total volume, at >90% purity by SDS–PAGE with Coomassie Blue staining). An aliquot (50 μL) of this fraction containing TcPAM (~80 μg) was added to 50 mM phosphate buffer solution (1 mL final volume, pH 8.5) containing 5% glycerol and (S)-α-phenylalanine (100 μM), and the solution was incubated at 31 °C for 1 h. The reaction was quenched with 6 N NaOH to adjust the pH to >10, and then ethyl chloroformate (100 μL) was added to N-acylate the phenylalanines. After 5 min, the solution was again

basified (pH > 10), a second batch of ethyl chloroformate (100 μL) was added, and the reaction was stirred for 5 min. After derivatization, the mixture was acidified to pH 2−3 with 6 N HCl and extracted with diethyl ether (2× 1 mL). The organic solvent was evaporated *in vacuo*, the residue was dissolved in ethyl acetate/methanol (3:1, v/v) (200 μL) [methanol was used to liberate diazomethane in the following step], and the solution was treated with excess (trimethylsilyl)diazomethane (∼5 μL) to make the methyl ester of the *N*-acyl amino acid. The production of (*R*)-β-phenylalanine was assessed by GC/EI-MS fragmentation analysis, and the relative abundances of the base peak fragment ions of the amino acid derivatives were compared to those of an authentic standard.

The fraction of protein that eluted from the nickel-nitrilotriacetic acid affinity column containing active *Tc*PAM (76 kDa) was exchanged with elution buffer (20 mM Tris-HCl, pH 7.5, 50 mM NaCl, and 5% glycerol) through several concentration/dilution cycles using a Centriprep centrifugal filter (30,000 MWCO, Millipore) to remove the 250 mM imidazole. The protein, concentrated to 1 mL, was loaded onto a precalibrated gel filtration chromatography column (Superdex 200 prep grade, GE Healthcare Life Sciences) connected to a Pharmacia FPLC system (comprising a Biotech Recorder 102, Pharmacia Pump P-500, and Liquid Chromatograph Controller LCC-500). *Tc*PAM was eluted at 1 mL/min with elution buffer and was isolated in two peaks, one with an elution volume consistent with that of a 150 kDa MW standard, considered to be a dimer, and a larger peak consistent with protein >300 kDa, likely a multimeric aggregate. Equimolar amounts of protein from each fraction (40 μg of the 150 kDa fraction and 80 μg of the >300 kDa fraction) were separately incubated with α-phenylalanine (100 μM) at 31 °C for 1 h. The amino acids were derivatized to their *N*-acyl methyl esters, as described earlier, and analyzed by GC/EI-MS fragmentation analysis. The aminomutase in the 150 kDa fraction had 3-fold higher activity than in the >300 kDa fraction; therefore, the fraction containing the dimer was used for the crystallographic study, loaded into a size-selective centrifugal filtration unit (30,000 MWCO), and concentrated to 10 mg/mL. The purity (>95%) of the concentrated enzyme was assessed by SDS−PAGE with Coomassie Blue staining, and the quantity was determined by the Bradford protein assay.

PAM Activity Assays. Pilot assays to test for enzyme activity and to identify productive substrates were conducted separately at 31 °C with 750 μg of wild-type *Tc*PAM or its mutant forms with an appropriate substrate (at 1 mM) in 50 mM phosphate buffer solution (pH 8.5) containing 5% glycerol. The reactions were quenched with 6 N HCl, the pH was adjusted to pH 2, and then internal standards (3*R*)-(3′-fluoro)-β-phenylalanine (at 20 μM) and *trans*-2′-methylcinnamic acid (at 20 μM) were added. The cinnamic acids were extracted into diethyl ether, the organic solvent was evaporated *in vacuo*, the residue was dissolved in ethyl acetate/methanol (3:1, v/v) (200 μL), and the solution was treated with a (trimethylsilyl)diazomethane dissolved in ether (∼5 μL) to convert the acids to their methyl esters. Each sample was separately analyzed by GC/EI-MS and quantified by linear regression analysis. The remaining aqueous fraction was adjusted to pH >10 with 6 N NaOH, and the amino acids were derivatized to their *N*-(ethoxycarbonyl) methyl esters, as before. Each sample was separately analyzed/quantified by GC/EI-MS; in brief, the relative amounts of the α- or β-amino acid were determined by linear regression analysis of the area of the base peak ion of the derivatized α- and β-amino acids generated in the

EI-MS. The peak area was converted to concentration by solving the corresponding linear equation, derived by plotting the area of the base peak ion (produced by the corresponding authentic standard) against concentration ranging from 0 to 1.5 mM.

The substrates α-phenylalanine, 3′- and 4′-methyl-α-phenylalanine, and styryl-α-alanine were incubated separately with wild-type *Tc*PAM and its point mutant (L104A, designated PAMeLA_104: **p**henylalanine **a**mino**m**utase **e**xchange **L**eu→ **A**la_104), to establish steady-state conditions with respect to a fixed protein concentration and time at 31 °C. Under steady-state conditions, each substrate at 10, 20, 40, 80, 150, 300, 500, and 750 μM was separately incubated with *Tc*PAM or PAMeLA_104 in triplicate, single stopped-time assays. Each of the products in the reaction mixture was derivatized to their *N*-(ethoxycarbonyl) methyl ester and then quantified by GC/EI-MS analysis, as described previously. The kinetic parameters (K_M and k_{cat}) were determined from the Hanes-Woolf plot (R^2 was typically >0.98), and the stereochemistry of enzyme-catalyzed products was assessed by chiral GC/MS analysis (Chirasil-D-Val column, Varian).[15]

Intramolecular Analysis of the *Tc*PAM Reaction. [^{15}N]Phenylalanine (98% enriched) (10 mM) and [ring, β-C-^{2}H$_6$]cinnamate acid (98% enriched) (10 mM) were incubated together with *Tc*PAM (100 μg) using standard conditions in 1-mL assays. The reaction was quenched, and the amino acids isotopomers were derivatized to their *N*-(ethoxycarbonyl) methyl esters, and the sample was analyzed by GC/EI-MS, as described previously. The configuration of the β-phenylalanine was assessed by chiral GC/EI-MS analysis (Chirasil-D-Val column, Varian), as before.

Crystallization and Substrate Soaking of the *Tc*PAM. A Crystal Gryphon nanodispenser (Art Robbins Instruments) was used to set up sitting drop vapor diffusion crystallography plates (Intelli-Plate from Art Robbins Instruments) comprising an array of crystallization conditions in 96-well format. Crystals were grown in a condition containing *Tc*PAM apoenzyme (0.4 μL) and a reservoir containing 0.4 μL of 100 mM HEPES, pH 7.0, 1.0 M LiCl, and 15% PEG 6000. Crystals formed in a drop that had been left undisturbed for 10 days at 20 °C. Cinnamic acid (1.3 mM) was added to the crystallization buffer solution for substrate soaking studies, and the *apo*-*Tc*PAM crystals were picked up from the sitting drops and soaked over a range of 3 to 10 h in the buffer containing cinnamate. No crystal cracking was visualized under the microscope. Crystals were then flash-frozen in liquid nitrogen after soaking in cryoprotectant (30% glycerol in the reservoir solution). The native X-ray diffraction intensity data were collected under a continuous stream of liquid nitrogen at 100 K on beamline 21-ID-D, LS-CAT (Argonne National Laboratory, Advanced Photon Source, Chicago, IL) at a wavelength of 1.0782 Å. The data were processed using the HKL2000 software package.[16]

Molecular Replacement, Refinement, and Structural Analysis. Phasing information was acquired by the molecular replacement method (Table 1). A homology model based on the structures of a phenylalanine ammonia lyase (PDB entry 1W27)[17] and a tyrosine aminomutase (PDB entry 2RJR)[18] was built by the SWISS-MODEL online server with the MIO moiety removed.[19] A molecular replacement solution was found using the constructed model as the search query in the MOLREP program in the CCP4 suite.[20] The solution consisted of two monomers in one asymmetric unit, and the presence of the MIO moiety (formed autocatalytically by condensation of

Ala-Ser-Gly) in the active site of each monomer was confirmed by the electron density map. This structural motif was edited into the PAM structure from the model structures above (1W27 and 2RJR). The monomer library file was generated with the Sketcher program in the CCP4 suite. Model building and structural analysis were performed with the COOT program (version 0.6.1).[21]

Within the active site of PAM, the electron density of (E)-cinnamic acid was identified, and the corresponding molecule was built in. Restrained refinement with the Refmac5 program (in the CCP4 suite) was used to improve the electron density map for the PAM structure bound to *trans*-cinnamate. The final model contained 1289 residues from the two molecules in the asymmetric unit, 277 water molecules, and one cinnamate molecule bound to the active site of each monomer.

■ RESULTS

Expression and Characterization of Recombinant PAM. *Tc*PAM cDNA was codon optimized for expression as a soluble His-tagged protein in *E. coli*, as described previously.[14] Subsequent purification of *Tc*PAM by nickel affinity and gel filtration chromatographies yielded protein of 76 kDa at >95% purity. In vitro assays of the purified protein and GC/EI-MS analysis of the
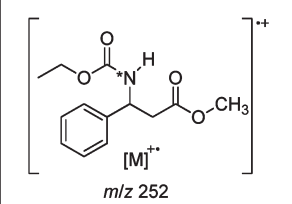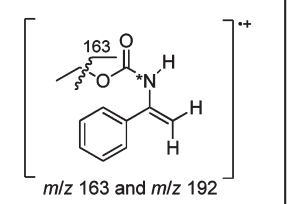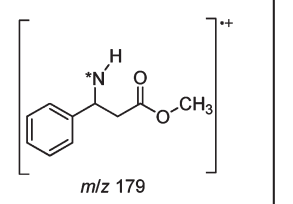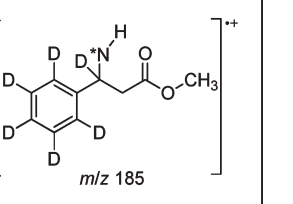
amino acid derivatives[14] confirmed that *Tc*PAM was functional. The *Tc*PAM reaction converts (S)-α-phenylalanine stereoselectively to (R)-β-phenylalanine.[22] The relatively high primary sequence homology of the active site residues between *Tc*PAM and *Sg*TAM (whose structure has been solved[12]) suggests that the locations of the residues would also be the same. However, *Tc*PAM preferentially catalyzes the formation of (3R)-β-phenylalanine, while the *Sg*TAM-catalyzed reaction forms (3S)-β-tyrosine of opposite stereochemistry; the observed differences in stereochemistry for these two aminomutases inferred that their active sites must be conformationally distinct. To assess this hypothesis, the crystal of a *Tc*PAM-cinnamate complex was obtained, and the three-dimensional structures of the *Tc*PAM and *Sg*TAM active sites were compared. This evaluation should begin to elucidate how *Tc*PAM directs the stereospecific detachment and rebound of the migratory amino group and hydrogen at C_β and C_α of the reaction intermediate.

Analysis of β-Phenylalanine Formed from the Incubation of *Tc*PAM with [^{15}N]Phenylalanine and [ring, β-C-^{2}H$_6$]Cinnamate Acid. Purified *Tc*PAM (200 μg) was incubated with a mixture of [^{15}N]phenylalanine and [ring, β-C-^{2}H$_6$]cinnamic acid (20 μmol of each). The α- and β-phenylalanine isotopomers were derivatized to their N-(ethoxycarbonyl) methyl esters, and cinnamic acid was converted to its methyl ester and analyzed by GC/EI-MS. Authentic standards of N-(ethoxycarbonyl)-β-phenylalanine methyl ester eluted from the GC column at 9.87 min. The mass spectrum of the derivatized biosynthetic β-phenylalanine ($\sim$200 nmol) isolated from the incubation allowed for quantitative analysis of the isotope enrichment and distribution. A molecular ion (M$^+$) of m/z = 252 indicated that the biocatalyzed product contained one extra mass unit compared to the mass of the unlabeled isotopomer (m/z = 251). The molecular ion and diagnostic fragment ions (base peak [M − CH$_3$CH$_2$-CO$_2$]$^+$ = 179, and lesser abundant ions m/z = 192 [M − HC(O)OCH$_3$]$^+$ and m/z = 163 [m/z 192 − CH$_3$CH$_2$]$^+$ (Table 2)) indicated that the additional mass unit was derived from the ^{15}N-atom. In addition, the ratio (10:1) of the ion abundance for the base peak m/z = 178 and m/z = 179 for authentic N-(ethoxycarbonyl)-β-phenylalanine methyl ester is identical to the calculated ratio of the base peak m/z = 179 and m/z = 180 of the N-(ethoxycarbonyl) methyl ester of the biosynthesized [^{15}N]-β-phenylalanine made after the incubation of *Tc*PAM with [^{15}N]phenylalanine and [ring, β-C-^{2}H$_6$]cinnamate acid. This suggested a ^{15}N enrichment of 98% and that no unlabeled β-phenylalanine derivative was present. A small percentage (<5%) of the biosynthetically derived β-phenylalanine contained seven additional mass units, according to a base peak fragment ion m/z = 185; the [^{15}N]-β-phenylalanine derivative was present at >95%. The isotopomer containing seven additional mass units was derived from the [ring, β-C-^{2}H$_6$]cinnamate

Table 1. Data-Collection and Structure-Refinement Statistics

	data collection
wavelength (Å)	1.0782
total reflection	250966
unique reflection	55249
space group	C 1 2 1
unit-cell parameters	a = 118.73, b = 76.11, c = 120.39 (Å)
	$\alpha = \gamma = 90°$, $\beta = 120.4°$
molecules per ASU	2
resolution range (Å)	2.38
completeness (%)	96.8 (79.6)
I/σ	18.8 (2.05)
R_{merge} (%)	10.1 (42.4)
	structure refinement
resolution (Å)	2.38
R_{cryst}/R_{free} (%)	0.1830/0.2392
	rmsd from ideal values
bond length (Å)	0.0097
bond angle (deg)	1.3102
average B factor	47.12
PDB #	3NZ4

Table 2. GC/EI-MS Analysis: Diagnostic Ions of Biosynthetic [^{15}N]-β-Phenylalanine[a]

m/z 252   *m/z* 163 and *m/z* 192   *m/z* 179   *m/z* 185

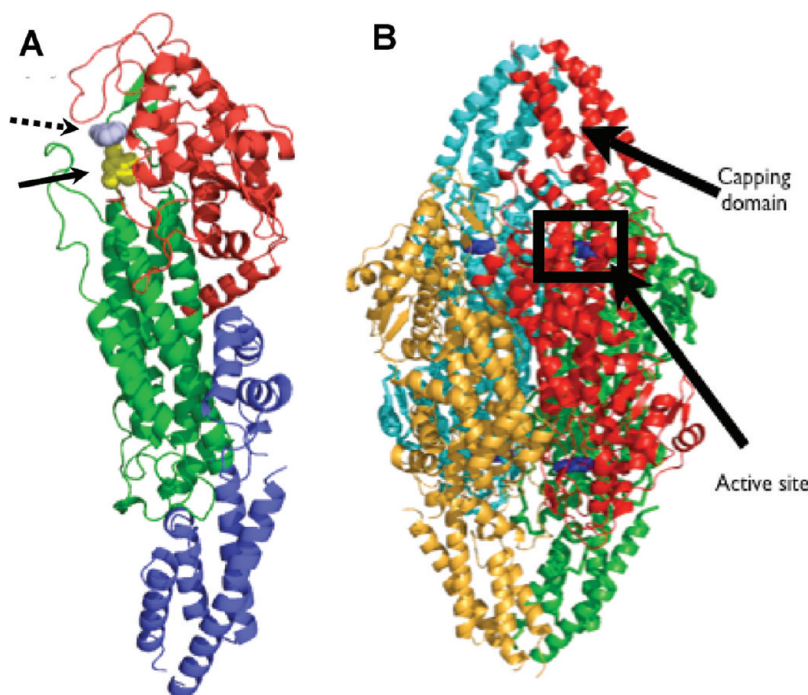[a] The asterisk (*) indicates the ^{15}N-atom.

Figure 2. Overall structure of PAM from *Taxus canadensis*. (A) A single monomer is shown and is colored by domain: N-terminal domain (red), central domain (green), and C-terminal domain (blue). The cinnamate molecule (light blue, designated with hashed arrow) and MIO (yellow, designated with solid arrow) are shown as space-filling spheres. (B) The PAM tetramer is shown, which can be seen as a dimer of two head-to-tail dimers resulting in a homotetramer with approximate 222-point symmetry. The subunits (red and orange) are related by a noncrystallographic 2-fold axis approximately perpendicular to the plane of the page, while the operation of a vertical crystallographic 2-fold axis produces the protomers (green and cyan) that complete the tetramer.

acid in the mixed substrate assay with *Tc*PAM and was not present in control assays where the labeled cinnamate acid was left out.

X-ray Crystal Structure Determination of *Tc*PAM. The *Tc*PAM structure was determined by molecular replacement using a search model derived by fitting the *Tc*PAM amino acid sequence to the published coordinates of PALs from *R. toruloides*[23] or *Sg*TAM from *S. globispora*.[12] *Tc*PAM shares the tertiary (Figure 2A) and quaternary (Figure 2B) structural features of the highly homologous and mechanistically similar members of the ammonia lyase family and *Sg*TAM (28−46% sequence identity), existing as a homotetramer.[12,17,23−26] In this study, *Tc*PAM was observed crystallographically as a tetramer with the protomers in the same relative orientation as observed for the PAL[17] and *Sg*TAM[12] tetramers.

Phenylalanine aminomutase from *Taxus chinensis* was shown to catalyze the conversion of the (*E*)-cinnamic acid substrate to enantiopure α- and β-phenylalanines when incubated in 6 M aqueous ammonium carbonate at pH 10, in a previous study; *cis*-cinnamic acid was shown to be a nonproductive substrate.[27] Thus, cinnamic acid was used as a co-crystallization substrate to assess the docking conformation of the phenylpropenoid skeleton within the *Tc*PAM active site relative to the position of the catalytic residues. The crystals of the aminomutase formed as small irregular polyhedra and belong to space group C2 with cell dimensions of $a = 118.7$ Å, $b = 76.1$ Å, and $c = 120.4$ Å; two 76 kDa monomers reside in the asymmetric unit, while a crystallographic 2-fold axis relates both halves of the tetramer. The final structure was refined to 2.38 Å (Figure S1, Supporting Information) with $R_{cryst}/R_{free} = 0.1883/0.2432$. Ramachandran

plots suggested that the numbers of disallowed residues were within the tolerance limit.

A (*E*)-cinnamate molecule (cf. Figure S1, Supporting Information, for density map) is bound in the active site, lying above the MIO and under a loop region that includes residues 80−97, which define the top of the active site (Figure 3A and B). The (*E*)-cinnamate molecule lies about 3.4 Å above the methylidene carbon of the MIO moiety. The carboxylate of the cinnamate makes a salt bridge interaction with a strongly conserved Arg-325, which serves to position the product in the active site. The plane of the aromatic ring of the cinnamate was observed to be displaced ∼20° from the perpendicular relative to the π-bond plane of the propenoate carbon−carbon double bond. The aromatic ring is bound relatively loosely in the active site, making only one direct hydrophobic interaction with Leu-104 (3.3 Å, not shown). The only other close contact between cinnamate and an active site residue is a 2.9 Å interaction between the hydroxyl of Tyr-80 and C_α of the cinnamate (Figure 3B).

Structural Characteristics of *Tc*PAM. The *Tc*PAM structure, like other MIO-based enzyme structures, contains a central domain made almost exclusively of α-helices that run mostly parallel to the long axis of the molecule (cf. Figure 2A). The center of the domain consists of a four-helix bundle surrounded mostly at its base by six additional α-helices that define the C-terminus of the monomer. An additional four-helix bundle domain resides at the bottom of the structure and contains an insertion of about 100 amino acids (residues 500−610 in *Tc*PAM) compared to closely related members in the class I lyase-like family. This structural domain is conserved in the PAL enzymes from plants but is
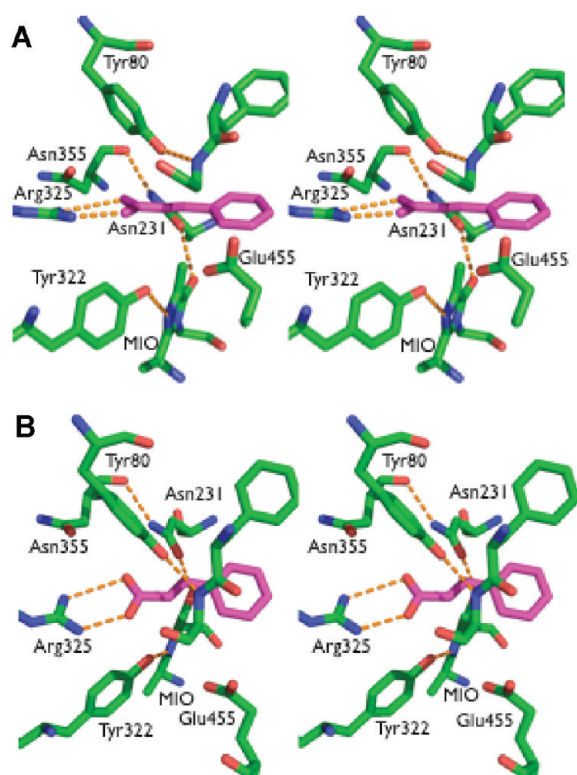
Figure 3. Stereoview of the *Tc*PAM active site-cinnamate complex (cyan). The PAM active site residues are colored by atom as follows: C (green), O (red), and N (blue). (A) Side view and (B) topside view.

absent in the structures of all other enzymes in the family isolated from different organisms.[24] The MIO moiety is located at the top of the four-helix bundle and is contained by the N-terminal domain, which is also almost exclusively α-helical and defines the top of the monomer. The active site is therefore located between the central and N-terminal domains and comprises amino acid residues from both domains. The oligomerization interface runs the length of the central and N-terminal domains, and numerous intersubunit interactions are evident in both domains, though the majority of the interface is contained within the central domain (Figure 2B). Contributions to the active site from adjacent subunits come from the bottom C-terminal end of the molecule. The interface buries 16756.7 Å^2 (74.36% of the total area), indicating a relatively strong oligomeric association. The active site is made up almost entirely of loop regions that surround the MIO moiety, and most of the residues that make up the active site are highly conserved in all the MIO-containing enzymes known (Figure S2, Supporting Information).

Site-Directed Mutation of an Active Site Leu of *Tc*PAM. As noted earlier, the *Tc*PAM-cinnamate complex shows that the 3′-carbon of the bound intermediate is close to the Leu-104 residue, likely involved in a van der Waals interaction with the substrate (Figure 4; Leu-104 of *Tc*PAM was changed to the Ala104-mutant and is designated as PAMeLA_104) to assess how this would affect the aminomutase reaction with sterically demanding non-natural substrates compared to the reaction with the wild-type enzyme. The kinetic parameters were obtained separately for *Tc*PAM with substrates 3′-methyl-α-phenylalanine, styryl-α-alanine, and 4′-methyl-α-phenylalanine and compared to those

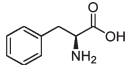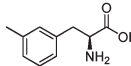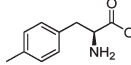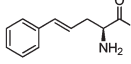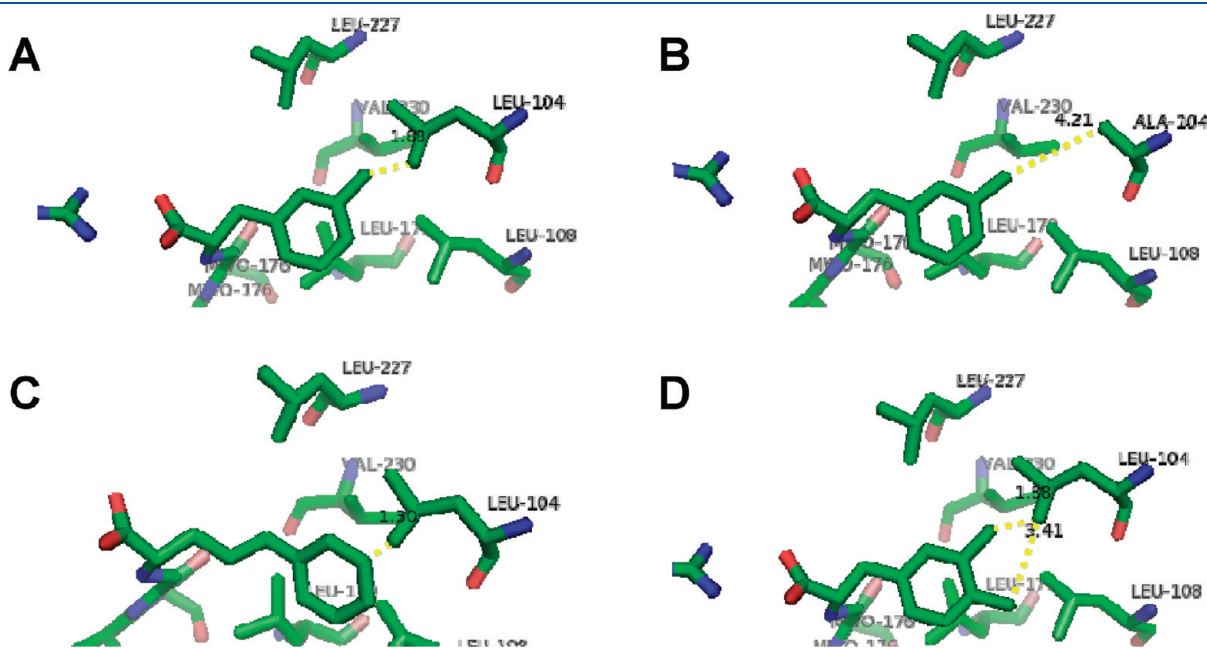**Figure 4.** The *Tc*PAM-cinnamate complex is used to approximate the trajectory of non-natural substrates. (A) The 3′-methylphenyl-α-alanine substrate is modeled into the active site of *Tc*PAM showing the distance (∼1.9 Å) between the 3′-methyl of the substrate and Leu-104, (B) the 3′-methylphenyl-α-alanine substrate is modeled into the mutant PAMeLA_104 active site where the steric volume is increased through the mutation of Leu-104 to Ala; now, the closest distance between the bound substrate and residue 104 is estimated at 4.2 Å, and (C) styryl-α-alanine modeled in the *Tc*PAM active site showing the hydrophobic interaction with Leu 104 at a distance of 1.3 Å. (D) 3′- and 4′-methyl-α-phenylalanine are superimposed and modeled in the *Tc*PAM active site. The relative positions of the methyl substituents on the phenyl ring of each substrate to Leu-104 are shown along with the distances (1.9 and 3.4 Å, respectively) between the δ-C of Leu-104 and 3′-methyl and 4′-methyl.

Table 3. Kinetic Parameters for _Tc_PAM and PAMeLA_104 with Various Substrates

	Substrate	Enzyme	K_M (M) ×10³	$^{\beta}k_{cat}$ (s⁻¹)[a]	$^{cin}k_{cat}$ (s⁻¹)[a]	$^{\beta}k_{cat}/K_M$ (M⁻¹·s⁻¹)	$^{cin}k_{cat}/K_M$ (M⁻¹·s⁻¹)	k_{cat}/K_M[b] (M⁻¹·s⁻¹)
1		_Tc_PAM	0.057 (±0.004)	0.053 (±0.01)	0.012 (±0.002)	930 (±20)	210 (±30)	1100 (±100)
		PAMeLA_104	0.136 (±0.002)	0.003 (<±0.001)	0.073 (±0.003)	22 (±2)	540 (<±10)	560 (±10)
2		_Tc_PAM	0.397 (±0.03)	0.022 (±0.002)	0.017 (±0.002)	55 (±7)	42 (±5)	48 (±20)
		PAMeLA_104	0.083 (±0.008)	0.028 (±0.003)	0.032 (±0.003)	340 (±50)	380 (±60)	720 (±20)
3		_Tc_PAM	0.091 (±0.005)	0.030 (±0.002)	0.005 (±0.002)	330 (±20)	55 (±3)	380 (±20)
		PAMeLA_104	0.073 (±0.005)	0.020 (±0.002)	0.017 (±0.002)	270 (±20)	230 (±20)	510 (±10)
4		_Tc_PAM	0.250 (±0.004)	<0.0002	0.082 (±0.002)	<1	330 (<±10)	330 (±10)
		PAMeLA_104	0.120 (±0.004)	0.003 (±0.002)	0.12 (<±0.01)	25 (±2)	1000 (±100)	1000 (±100)

[a] The terms $^{\beta}k_{cat}$ and $^{cin}k_{cat}$ represent the kinetic constants for the formation of the β-arylalanines and _trans_-arylacrylates, respectively. [b] The kinetic constant $k_{cat} = {}^{\beta}k_{cat} + {}^{cin}k_{cat}$. α-Phenylalanine (**1**), 3′-methyl-α-phenylalanine (**2**), 4′-methyl-α-phenylalanine (**3**), and styryl-α-alanine (**4**) at steady-state. Standard errors are in parentheses.

obtained for PAMeLA_104 in parallel enzyme assays with the same substrates (Table 3).

Notably, β-phenylalanine and _trans_-cinnamate are products of the _Tc_PAM reaction when phenylalanine is used as the substrate,[3] and therefore, the sum of their production rates at steady-state was used to calculate the turnover rate (k_{cat}) of all the products (Table 3). The catalytic efficiency (k_{cat}/K_M) of _Tc_PAM and PAMeLA_104 for the natural substrate α-phenylalanine **1** is 1100 M⁻¹·s⁻¹ and 560 M⁻¹·s⁻¹, respectively. The product distribution of the _Tc_PAM reaction, after 30 min, was dominated by β-phenylalanine, made at 0.053 s⁻¹, and cinnamate was made more slowly at 0.012 s⁻¹. Reciprocally, the product pool of the PAMeLA_104 reaction with **1** principally contained cinnamate, which was made at a rate of 0.073 s⁻¹, while the β-amino acid was made fractionally at 0.003 s⁻¹.

The catalytic efficiency of _Tc_PAM and PAMeLA_104 for 3′-methylphenyl-α-alanine (**2**) is 48 M⁻¹·s⁻¹ and 720 M⁻¹·s⁻¹, respectively. The increase in catalytic efficiency for substrate **2** is due largely to the ~5-fold decrease in K_M of PAMeLA_104 (83 μM) compared to the K_M of _Tc_PAM (397 μM). The distribution of the 3′-methyl-β-phenylalanine and 3′-methylcinnamate was at ~1:1 for both PAMeLA_104 and _Tc_PAM catalysis; however, the combined rate of formation of both 3′-methyl-β-phenylalanine and 3′-methylcinnamate by PAMeLA_104 (0.060 s⁻¹) is slightly increased compared to the rate of the same reaction by _Tc_PAM (0.039 s⁻¹) (Table 3).

Interestingly, both _Tc_PAM ($k_{cat} = 0.035$ s⁻¹) and PAMeLA_104 ($k_{cat} = 0.037$ s⁻¹) were kinetically similar when 4′-methyl-α-phenylalanine (**3**) was used as the substrate, and their K_M values, 91 μM and 73 μM, respectively, were also comparable as well as their catalytic efficiency values (380 M⁻¹·s⁻¹ and 510 M⁻¹·s⁻¹ (Table 3)). However, the rates of formation of the 4′-methyl-β-phenylalanine and 4′-methylcinnamate products (0.030 s⁻¹ and 0.005 s⁻¹, respectively) catalyzed by _Tc_PAM from **3** were significantly different from the respective distribution catalyzed by PAMeLA_104 (0.020 s⁻¹ and 0.017 s⁻¹).

_Tc_PAM was incubated with styryl-α-alanine (**4**) and rapidly catalyzed the exclusive conversion of **4** to the corresponding 5-phenyl-(2_E_,4_E_)-pentadienoate (i.e., (_E_,_E_)-styrylacrylate) at 0.082 s⁻¹ and styryl-β-alanine at <0.0002 s⁻¹ (Table 3). Comparatively, PAMeLA_104 converted **4** to the corresponding

(_E_,_E_)-styrylacrylate faster, at 0.12 s⁻¹; however, styryl-β-alanine was produced significantly faster by PAMeLA_104 than by _Tc_PAM, yet still at a slow rate of 0.003 s⁻¹. It is worth noting that the Michaelis constants for both _Tc_PAM and PAMeLA_104 are 250 μM and 120 μM, respectively, for the styryl-α-alanine substrate, suggesting that the L104A mutation is able to enhance the binding affinity for **4** and thus contributes toward increasing the overall catalytic efficiency from 330 M⁻¹·s⁻¹ for _Tc_PAM to 1000 M⁻¹·s⁻¹ for PAMeLA_104.

Preliminary Mutagenesis of the Putative Catalytic Residue of _Tc_PAM. A previous evaluation of the structure and mechanism of the MIO-dependent ammonia lyases[17,23−26] and a tyrosine aminomutase[12] revealed several active site residues proposed for substrate binding and MIO-charge management. Of interest, a conserved Tyr residue present in all members of the lyase family (cf. Figure S2, Supporting Information, Tyr-80 in _Tc_PAM) has been proposed to serve as the catalytic base.[9,18,25] It is postulated that the conserved Tyr removes a prochiral hydrogen at C_β of the arylpropanoid substrates in the lyase and mutase reactions. Thus, Tyr-80 in _Tc_PAM was targeted as the general base; the hydroxyl group of this residue is close to the C_α and C_β of the bound cinnamate molecule (Figure 5A). The function of Tyr-80 in _Tc_PAM was assessed herein by characterizing a Y80F mutant, which when incubated with α-phenylalanine did not produce detectable β-phenylalanine nor _trans_-cinnamate compared to the wild-type enzyme. In previous reports, analogous Tyr mutants of HAL and PAL also displayed dramatic reduction in catalytic activity.[28,29]

■ DISCUSSION

Course of MIO-Dependent Enzyme Reaction Mechanisms. Structures have been determined for several members of this lyase class I-like family, including HAL from _Pseudomonas putida_,[26] TAL from _Rhodobacter sphaeroides_ (_Rs_TAL),[25] PALs from _Anabaena variabilis_,[24] _Nostoc punctiforme_,[24] _Rhodosporidium toruloides_,[23] and _Petroselinum crispum_,[17] and _Sg_TAM.[12] All have very similar overall folds, contain MIOs imbedded in an active site of similar overall architecture, and exist as homotetramers. In most structures, two of the subunits significantly contribute active site residues, and a third subunit encapsulates one side
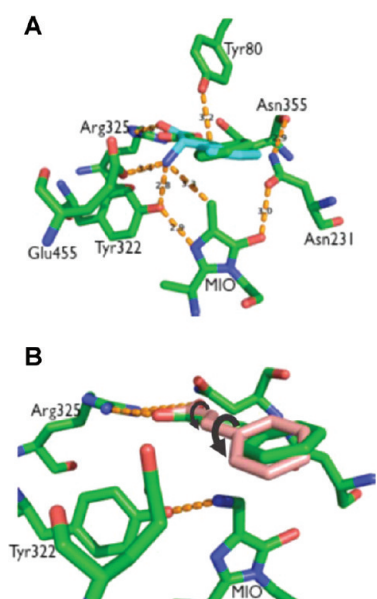
Figure 5. Modeling of the reaction pathway. (A) Using the atom color scheme as described in Figure 3 (except for the carbon atoms of the phenylalanine substrate, which are cyan), phenylalanine is modeled in the active site based on the structure of the TcPAM-cinnamate complex; cinnamate is superimposed. (B) Two conformations of cinnamate are shown; the initial bound structure (green carbon atoms) and the postulated conformation after rotating about the C_1-C_α and $C_{ipso}-C_\beta$ bonds by 180°. (C) The β-phenylalanine-MIO intermediate is modeled in the TcPAM active site showing a potential interaction between Glu455 and the amino group.

of the active site, while in SgTAM, this third subunit contributes residues that interact with the substrate. In recent studies, α- and/or β-tyrosine mimics were covalently trapped in the active sites of SgTAM[18] and RsTAL,[25] and their structures were determined, demonstrating that the amino group of the substrate attacks the MIO of this aminomutase. The SgTAM structures bound to the substrate or product mimics show that a nucleophile at either C_α or C_β will attack the MIO moiety.[9,18] These results have shed considerable light on the mechanism of the MIO-based catalysts, countering previous work inferring that the MIO couples as an electrophile to the aromatic ring of the substrate to activate catalysis.[30]

Stereochemical Course of the TcPAM Reaction. In earlier studies, the stereochemical evaluation of the ammonia lyase reactions included an assessment of the stereoselectivity, showing universally that the *trans*-diastereomer of the acrylate product is made exclusively upon elimination of ammonia[31] and that one prochiral hydrogen at C3 is stereospecifically removed from the substrate during the process.[32,33] SgTAM of bacterial origin and TcPAM of plant origin are the only aminomutases in the class I ammonia lyase-like family whose structures are known, and the reaction stereochemistry of the aminomutases have been evaluated. The SgTAM reaction was found to make (3S)-β-tyrosine; the mode of transfer (inversion or retention of configuration and intra- or intermolecular group transfer) was not evaluated.[9,12] However, evaluation of the cryptic components of the TcPAM reaction has shown that the amino group and hydrogen are removed from the substrate, their positions exchanged, and then both are reattached *intra*molecularly to the original carbon scaffold (as confirmed herein) with retention of configuration.

The results of the mixed substrate assay containing [ring, β-C-^{2}H$_6$]cinnamate and [^{15}N]phenylalanine indicate that the nitrogen migrates quantitatively from the α- to the β-carbon with negligible exchange to exogenously supplied cinnamate molecules at a concentration (10 mM) likely much higher than physiological levels. TcPAM maintains high fidelity with the natural phenylalanine substrate through tight binding of the substrate and reaction intermediate, at the exclusion of competitive substrates, in order to achieve the observed reaction efficiency.

Evidence for Substrate Rotation in the TcPAM Active Site. Despite the wealth of structural data collected on this family of enzymes with overall very similar active site architecture, none sheds any light to explain how the stereochemistry of the TcPAM reaction proceeds with retention of configuration and makes the (3R)-β-phenylalanine isomer, which is opposite to the (3S)-stereochemistry found in the product of the SgTAM reaction. Therefore, a favorable binding conformation of the (E)-cinnamate substrate in the TcPAM-cinnamate complex (see Figure 3B) was used as a basis to understand how these aminomutases produce β-amino acids of opposite stereochemistry. The product of the TcPAM reaction is proposed to be made from phenylalanine via a concerted Hoffman-like elimination reaction during the reaction cycle.[3] The catalytic base Tyr-80 is situated above the $C_\alpha-C_\beta$ bond of the bound phenylalanine substrate (in a staggered conformation), with the *pro*-(3S) hydrogen closest to Tyr-80 (Figure 5A); the MIO moiety is positioned below the $C_\alpha-C_\beta$ bond of the substrate, with the amino group proximate to the methylidene of the MIO. The formation of the transoid acrylate product supports the stereoselective removal of the *pro*-(3S) proton by a *Taxus* PAM, described previously.[8]

However, for the production of (R)-β-phenylalanine, the mechanism of catalysis must adhere to an intramolecular amino group transfer, where the amino group does not exchange with that from another substrate molecule.[8] In addition, the stereochemistry must account for the retention of configuration at the migration termini.[22] These data suggest that the amino group and hydrogen displaced from the (2S)-α-phenylalanine substrate must rebind, respectively, at C_β and C_α of the (E)-cinnamate before it diffuses from the active site. The constraints of the intramolecularity and stereochemistry of the TcPAM reaction present a challenge because the amino group must attach to the cinnamate on the side facing opposite to that of the NH$_2$-MIO intermediate (cf. Figure 3A) to produce the (R)-product. Since this stereochemistry is opposite to the (S)-β-tyrosine product made by SgTAM, the covalent intermediate derived by reacting SgTAM with a product analogue having the configuration at C_β as the natural (S)-β-product is not representative of the TcPAM reaction stereochemistry.

In the SgTAM reaction, the amino group can migrate from C_α to C_β across the same face of the coumarate intermediate to isomerize (S)-α- to (S)-β-tyrosine.[9,18] In contrast, for the TcPAM reaction, the C_α-amino group must be removed from the *re*-face (using C_β of the cinnamate intermediate as reference), then reattach at C_β on the opposite face (cf. Figure 1). A possible explanation involves approximately 180° rotations of the already-bound cinnamate intermediate about both the C_1-C_α and $C_{ipso}-C_\beta$ bonds prior to rebound of the amino group to C_β by the NH$_2$-MIO (Figure 5B), without breaking the salt bridge to Arg-325, and with minor displacement of the aromatic ring from its original position (Figure 6 and cf. Figure 5B). This rotamer
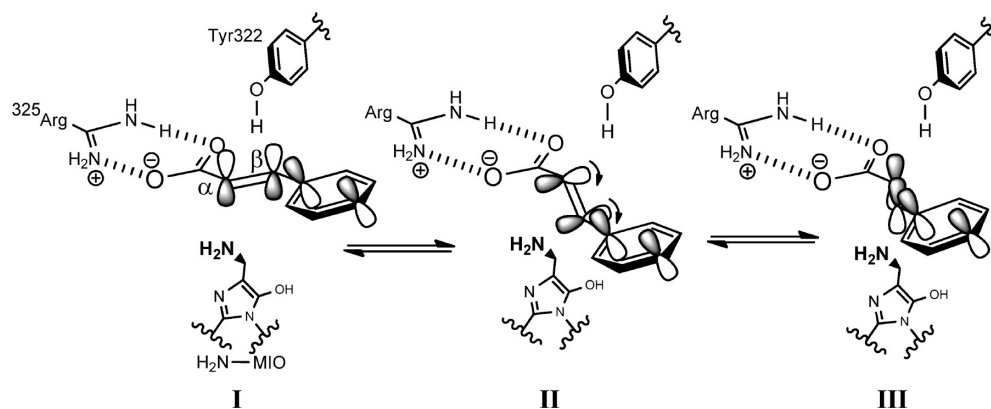
Figure 6. Shown is a rendering of the *in situ* progression of one near-planar rotamer of (*E*)-cinnamate (**I**) in the *Tc*PAM active site to the other (**III**) via a midpoint rotational intermediate (**II**). Key catalytic residues are included, and their relative positions are based on those in the *Tc*PAM structure: Arg-325 forms a salt bridge with the carboxylate of cinnamate, Tyr-80 is the presumed catalytic base, situated "above" the cinnamate, and the NH_2-MIO complex is shown, "below" the cinnamate. For rotamer **I**, the NH_2 of NH_2-MIO is closer to C_α, while for rotamer **III**, NH_2 is closer to C_β and faces the opposite side of the cinnamate. The *p*-orbitals on the C=C and the ring are provided for the perspective of rotation. In particular, the lobes of the orbitals on the ring remain oriented in the same direction, while those on the acrylate rotate about the C_1-C_α and $C_{ipso}-C_\beta$ bonds.

positions C_β for nucleophilic attack by the NH_2-MIO moiety to form the enzyme/product covalent intermediate. Tyr-80 is in position on the opposite side to reprotonate the phenylpropanoid at C_α, resulting in overall retention of configuration in the product. The nitrogen linking the MIO to the product is likely protonated by Tyr-322 that initiates the departure of the product from the MIO (Figure 5A). Concomitant rotation about the C_1-C_α and $C_{ipso}-C_\beta$ bonds does not result in any steric clashes in the active site, nor in breaking direct interactions between enzyme and substrate. The foregoing proposed mechanism is consistent with all of the stereochemical and mechanistic findings for *Tc*PAM. In addition, the $K_{eq} \sim 1$ for the *Tc*PAM reaction[22] suggests that the rotamers are energetically equivalent.

The orientation of the (*S*)-α-amino acid in the active site of *Tc*PAM is determined by the direction of the carboxylate group when it forms a salt bridge with the δ-guanidino group of a proximate Arg-325, as in the *Tc*PAM-cinnamate complex and all other bound structures of enzymes from the lyase-like family.[12,17,23−26] In previous investigations, assessing the stereochemical course of the *Tc*PAM reaction in the absence of structural data, it was suggested that the differences in the stereochemistry of the *Tc*PAM reaction compared to that of the *Sg*TAM reaction resulted from fundamental differences in the active sites of these isomerases. The substrate was hypothesized to bind the *Tc*PAM active site with the carboxylate and phenyl ring in a *syn*-periplanar orientation to position the migrating H and NH_2 groups of the (*S*)-phenylalanine on the same side of the molecule to account for the retention of configuration at the reaction termini.[22] Shown herein, however, the active site of *Tc*PAM is arranged similar to the other MIO-dependent enzymes, where the catalytic base and MIO (amino group acceptor) are antipodal with respect to the substrate; thus, the migration of the H and NH_2 groups must also occur on opposite sides. Consequently, a *syn*-periplanar orientation or *cis*-cinnamate configuration of a reactive intermediate would confound the observed retention of stereochemical configuration of the *Tc*PAM reaction. More importantly, a cisoid phenylpropanoid (either as *s-cis*-phenylalanine or *cis*-cinnamate) in a modeled complex with *Tc*PAM would be sterically occluded by several active site residues (Figure S3, Supporting Information). Further,
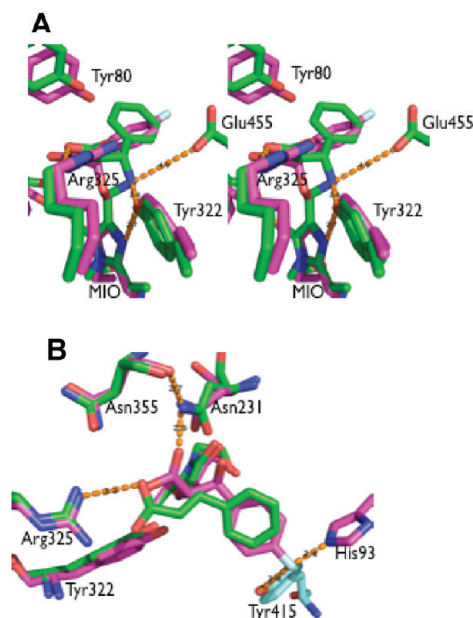

Figure 7. Comparison of the *Tc*PAM and *Sg*TAM active sites. (A) Stereoview of the active sites showing a *Tc*PAM-cinnamate complex and a *Sg*TAM-2,3-dihydroxy-(*para*-fluoro)phenylpropanoid complex overlaid on their MIO-groups; the latter complex was derived from *para*-fluorocinnamate epoxide. The epoxide attacked the MIO (Lewis acid) likely forming an oxonium, and then was ring-opened nucleophilically by H_2O at the β-carbon to yield the dihydroxy derivative covalently attached to the MIO via ether linkage. Atoms are colored accordingly: carbon atoms of the *Tc*PAM complex (green) and carbon atoms of *Sg*TAM (magenta). (B) "Side" view of the *Sg*TAM-2,3-dihydroxy-(*para*-fluoro)phenylpropanoid complex overlaid on the *Tc*PAM-cinnamate complex.

electron density consistent with a (*E*)-cinnamate is clearly observed in the *Tc*PAM structure and provides good evidence that the reaction proceeds via a transoid intermediate.

Differences in Substrate Trajectory in *Sg*TAM and *Tc*PAM. The active sites of *Sg*TAM and *Tc*PAM were overlaid with the

MIO groups superimposed (Figure 6A and B). The salt bridge to Arg-325 involving both oxygens of the cinnamate in TcPAM is replaced in SgTAM by a much weaker interaction with the Arg (3.2−3.4 Å) and a strong interaction with Asn-205 (Asn-231 in TcPAM), which is proposed to also stabilize the protonated enol of the MIO (cf. Figure 1). Consequently, the carboxylate of the SgTAM substrate is placed proximate to the amine at C_β, as seen in both SgTAM/product-mimic structures.[18] The hydrogen bonds made by His-93 and Tyr-415 (which comes from the third protomer in the SgTAM tetramer) to the hydroxyl group of the tyrosine substrate lead to rotation of the aromatic ring of the substrate by about 40° relative to that of the ring of the cinnamate substrate in TcPAM, causing a change in the trajectory of each substrate through its corresponding active site. This altered substrate docking in the SgTAM active site enables the C_{MIO}-N bond of the NH_2-MIO intermediate to rotate and position the amino group near C_β of the acrylate intermediate. Interestingly, two distinct regions in the SgTAM active site are used to perform amination chemistry; at one location, the amino group is transferred from the substrate to the MIO, and at the other location via C_{MIO}-N bond rotation, the amino group is transferred from the MIO to the substrate. These MIO-rotamers in SgTAM are also required to give the stereochemistry observed in the product. In TcPAM, however, the transfer of the amino group to and from the MIO occurs in the same location. Thus, the different rotamers of the bound cinnamic acid in TcPAM, described in the previous section, must place either the C_α or the C_β proximate to the amino group of the NH_2-MIO complex, and rebound of the amino group to the appropriate phenylpropenoid rotamer establishes whether α- or β-phenylalanine is produced. Consequently, the resultant altered trajectory of the substrate through the active site in TcPAM versus SgTAM (Figure 7A and B) may contribute to the different stereochemical outcomes of the two enzymes. However, it must be pointed out that while the substrate/intermediate cinnamate is bound in the TcPAM, covalent intermediates are bound in SgTAM, which may also contribute to the differences in trajectory.

Effects of L104A Point Mutation on Enzymatic Activity. In this study, the effect of a targeted point mutation on substrate selectivity and enzymatic reactivity were investigated for the $Taxus$ phenylalanine aminomutase. The structure of TcPAM revealed that Leu-104 makes a direct hydrophobic interaction with the aromatic ring (nearest the 3′-carbon) of the presumed reaction intermediate cinnamate. Mutation of this Leu-104 to a sterically smaller alanine residue was proposed to increase the active site volume, reduce a steric interaction between the substrate and the active site, and thus increase the catalytic efficiency of the catalyst for arylalanine substrates bearing a substituent on the 3′-carbon of the ring. For proof of principle, sterically demanding substrates 3′-methyl-α-phenyl-, 4′-methyl-α-phenyl-, and styryl-α-alanine were chosen to evaluate the effects of the L104A mutation in TcPAM (PAMeLA_104).

In a previous investigation, TcPAM was found to generally isomerize α-arylalanines to their corresponding β-arylalanines; however, the catalytic efficiency of TcPAM decreased markedly with increasing steric bulk on the α-amino acid substrate.[15] Thus, the steric hindrance of the active site seemingly limited its catalytic efficiency. Kinetic parameters of the PAMeLA_104 enzyme with non-natural aryl amino acids were compared to the TcPAM catalyst, demonstrating that Leu-104 has significant influence on substrate binding (approximated by K_M), product

distribution, and k_{cat}. Notably, the K_M of PAMeLA_104 increases over 2-fold with the phenylalanine substrate (**1**) compared to the K_M of TcPAM, suggesting that Arg-325 and Leu-104 participate in substrate docking via a salt bridge and hydrophobic interaction, respectively.

PAMeLA_104 released total product (β-phenylalanine and cinnamate) at a rate (k_{cat} = 0.076 s^{-1}) comparable to that of TcPAM (k_{cat} = 0.065 s^{-1}) but produced (∼6-fold) more cinnamate than β-phenylalanine (cf. Table 3). Likely, an accessible orientation of phenylalanine in the mutant causes the reaction to stall after the first reaction step and release the acrylate product. Apparently, this orientation is not achievable in TcPAM, which preferentially makes β-phenylalanine. In contrast, the K_M of PAMeLA_104 was nearly 5-fold lower with 3′-methyl-α-phenylalanine (**2**) compared to the K_M of TcPAM, suggesting that the 3′-methyl substituent of the substrate enhanced substrate binding in the mutant. While the Leu→Ala exchange likely reduced unfavorable steric strain (cf. Figure 4A), the smaller alanine residue, however, could still make a constructive hydrophobic interaction with the 3′-methyl group of **2** (cf. Figure 4B). Remarkably, the catalytic efficiency of PAMeLA_104 for **2** increased ∼7-fold compared to TcPAM catalysis, which is primarily a reflection of the considerable (5-fold) reduction in K_M (i.e., better binding) of PAMeLA_104 compared to that of TcPAM.

While TcPAM and PAMeLA_104 displayed dramatic differences in their kinetic parameters with α-phenylalanine and 3′-methyl-α-phenylalanine, they did not display significant differences with 4′-methyl-α-phenylalanine (**3**). The K_M of TcPAM with substrate **3** was 1.6-fold higher than that for TcPAM with its natural substrate **1**, suggesting that the 4′-methyl group of the substrate only modestly affected binding. Interestingly, the K_M of PAMeLA_104 for **3** was slightly lower than that of TcPAM, suggesting that the Leu→Ala replacement likely enabled the 4′-methylphenyl functional group to adopt a suitable conformation to interact favorably with other distal hydrophobic residues (Leu-179, Leu-227, and Val-230) of the active site pocket (cf. Figure 4D). Moreover, the structural data for TcPAM shows no active site residues proximate to the 4′-carbon of the natural substrate that would interfere sterically with a 4′-alkyl substituent of **3**.

TcPAM converted styryl-α-alanine (**4**) almost exclusively to (E,E)-styrylacrylate, while PAMeLA_104 made the corresponding β-amino acid from **4**, albeit slowly, at about 3% of the styrylacrylate production rate at 0.12 s^{-1}. The wild-type and mutant enzymes made the styrylacrylate product from **4** faster than they were able to convert any of the other aryl amino acid substrates to their corresponding β-amino acids and acrylate products combined (cf. Table 3). These data suggest that the ammonia lyase function of both enzymes remains largely efficient with **4**. The stability of the conjugated π-bonds and the larger steric volume of the product, likely effected the rapid release of the intermediate, reducing the residence time needed to isomerize the α- to β-amino acid. PAMeLA_104 noticeably made more styryl-β-alanine than does TcPAM under steady-state conditions, indicating that the mutation likely increased the residence time of the substrate and ensuing intermediate in the active site. The 2-fold lower K_M of PAMeLA_104 compared to that of TcPAM for substrate **4** demonstrates that the mutant can accommodate **4** better. (cf. Figure 4C).

Clearly, the hydrophobic region of the TcPAM active site surrounding the aromatic ring of the purported reaction

intermediate (cinnamate) plays a major, but mechanistically unknown, role in substrate selectivity and in governing the distribution of the intermediate acrylic acid that is released and is converted to the β-amino acid.

Concluding Remarks. The structure of the phenylalanine aminomutase on the Taxol biosynthetic pathway[11,34] has been presented. The *Tc*PAM active site was observed to be arranged similar to that of other members of the MIO-dependent family of enzymes. The (3*S*)-product stereochemistry catalyzed by the bacterial *Sg*TAM and *Pa*PAM[3] is opposite to the (3*R*)-product stereochemistry catalyzed by *Tc*PAM of plant origin. Conceptually, the stereochemistry of the *Tc*PAM reaction can be achieved by rotation of the intermediate cinnamate in the active site by approximately 180° about the $C_1–C_\alpha/C_{ipso}–C_\beta$ bonds prior to rebinding of the amino group at the β-position on the (*E*)-phenylacrylate intermediate. Comparing the active sites of *Tc*PAM and *Sg*TAM showed subtle structural differences that may account for the significant changes in the orientation of the substrate, possibly causing stereodifferentiation.

On the basis of the *Tc*PAM crystal structure complex, the PAMeLA_104 mutant was constructed and demonstrated superior catalytic efficiencies for substrates 3′-methyl-α-phenylalanine and styryl-α-alanine possessing larger molecular steric volume. The L104A mutation likely reduced unfavorable steric clash that conceivably created an altered alignment of the substrate and/or the ensuing acrylate intermediate within the active site that changed the kinetic parameters of PAMeLA_104 compared to the wild-type *Tc*PAM.

This investigation of the *Tc*PAM structure provides a solid framework for further research into the details of stereochemical control in this enzyme that will require a combination of biochemical, synthetic, and structural approaches, with the eventual goal of both improving and rationally manipulating the enzyme for increased production of β-amino acids, *all-trans*-styrylacrylates, and paclitaxel and its analogues. Furthermore, the ability of *Tc*PAM to catalyze the production of aryl-β-amino acids via the isomerization of non-natural aryl-α-amino acids and through the addition of NH_3 to non-natural arylacrylate[27] supports its potential use as a biocatalyst.

■ ASSOCIATED CONTENT

Ⓢ Supporting Information. *Tc*PAM density map, amino acid sequence comparison of lyase family members, and *cis*-cinnamate modeled in the *Tc*PAM active site. This material is available free of charge via the Internet at http://pubs.acs.org.

■ AUTHOR INFORMATION

Corresponding Author
*Tel: (517) 355-9715. Fax: (517) 353 1793. E-mail: geiger@chemistry.msu.edu (J.G.); walker@chemistry.msu.edu (K.D.W.).

Author Contributions
§These authors contributed equally to this work.

■ ABBREVIATIONS

ASU, asymmetric unit; *E. coli*, *Escherichia coli*; GC/EI-MS, gas chromatography/electron impact mass spectrometry; HEPES, 4-(2-hydroxyethyl)-1-piperazineethanesulfonic acid; IPTG, isopropyl β-D-1-thiogalactopyranoside; MWCO, molecular weight cutoff; MIO, 3,5-dihydro-5-methylidene-4*H*-imidazol-4-one; PEG, polyethylene glycol; PAL, phenylalanine ammonia lyase; PAMeLA_104, phenylalanine aminomutase exchange Leu→Ala 104; PDB, protein databank; SDS—PAGE, sodium dodecyl sulfate—polyacrylamide gel electrophoresis; *Sg*TAM, tyrosine aminomutase from *Streptomyces globisporus*; *Rs*TAL, tyrosine ammonia lyase from *Rhodobacter sphaeroides*; *Taxus* PAM, phenylalanine aminomutase from source other than *Taxus canadensis*; *Tc*PAM, phenylalanine aminomutase from *Taxus canadensis*; Tris-HCl, tris(hydroxymethyl)aminomethane-hydrogen chloride; rmsd, root-mean-square deviation.

■ REFERENCES

(1) Christenson, S. D., Liu, W., Toney, M. D., and Shen, B. (2003) A novel 4-methylideneimidazole-5-one-containing tyrosine aminomutase in enediyne antitumor antibiotic C-1027 biosynthesis. *J. Am. Chem. Soc.* 125, 6062–6063.

(2) Krug, D., and Mueller, R. (2009) Discovery of additional members of the tyrosine aminomutase enzyme family and the mutational analysis of CmdF. *ChemBioChem* 10, 741–750.

(3) Walker, K. D., Klettke, K., Akiyama, T., and Croteau, R. (2004) Cloning, heterologous expression, and characterization of a phenylalanine aminomutase involved in Taxol biosynthesis. *J. Biol. Chem.* 279, 53947–53954.

(4) Poppe, L. (2001) Methylidene-imidazolone: a novel electrophile for substrate activation. *Curr. Opin. Chem. Biol.* 5, 512–524.

(5) Poppe, L., and Rétey, J. (2005) Friedel-Crafts-type mechanism for the enzymatic elimination of ammonia from histidine and phenylalanine. *Angew. Chem., Int. Ed.* 44, 3668–3688.

(6) Cooke, H. A., and Bruner, S. D. (2010) Probing the active site of MIO-dependent aminomutases, key catalysts in the biosynthesis of β-amino acids incorporated in secondary metabolites. *Biopolymers* 93, 802–810.

(7) Christenson, S. D., Wu, W., Spies, M. A., Shen, B., and Toney, M. D. (2003) Kinetic analysis of the 4-methylideneimidazole-5-one-containing tyrosine aminomutase in enediyne antitumor antibiotic C-1027 biosynthesis. *Biochemistry* 42, 12708–12718.

(8) Walker, K. D., and Floss, H. G. (1998) Detection of a phenylalanine aminomutase in cell-free extracts of *Taxus brevifolia* and preliminary characterization of its reaction. *J. Am. Chem. Soc.* 120, 5333–5334.

(9) Christianson, C. V., Montavon, T. J., Festin, G. M., Cooke, H. A., Shen, B., and Bruner, S. D. (2007) The mechanism of MIO-based

aminomutases in β-amino acid biosynthesis. *J. Am. Chem. Soc.* 129, 15744–15745.

(10) Wu, B., Szymanski, W., Wietzes, P., de Wildeman, S., Poelarends, G. J., Feringa, B. L., and Janssen, D. B. (2009) Enzymatic synthesis of enantiopure alpha- and beta-amino acids by phenylalanine aminomutase-catalysed amination of cinnamic acid derivatives. *ChemBioChem* 10, 338–344.

(11) Koksal, M., Jin, Y. H., Coates, R. M., Croteau, R., and Christianson, D. W. (2011) Taxadiene synthase structure and evolution of modular architecture in terpene biosynthesis. *Nature 469*, 116–U138.

(12) Christianson, C. V., Montavon, T. J., Van Lanen, S. G., Shen, B., and Bruner, S. D. (2007) The structure of L-tyrosine 2,3-aminomutase from the C-1027 enediyne antitumor antibiotic biosynthetic pathway. *Biochemistry 46*, 7205–7214.

(13) Ege, M., and Wanner, K. T. (2004) Synthesis of β-amino acids based on oxidative cleavage of dihydropyridone derivatives. *Org. Lett.* 6, 3553–3556.

(14) Cox, B. M., Bilsborrow, J. B., and Walker, K. D. (2009) Enhanced conversion of racemic α-arylalanines to (R)-β-arylalanines by coupled racemase/aminomutase catalysis. *J. Org. Chem. 74*, 6953–6959.

(15) Klettke, K. L., Sanyal, S., Mutatu, W., and Walker, K. D. (2007) β-Styryl- and β-aryl-β-alanine products of phenylalanine aminomutase catalysis. *J. Am. Chem. Soc. 129*, 6988–6989.

(16) Otwinowski, Z., and Minor, W. (1997) Processing of X-ray diffraction data collected in oscillation mode. *Method Enzymol.* 276, 307–326.

(17) Ritter, H., and Schulz, G. E. (2004) Structural basis for the entrance into the phenylpropanoid metabolism catalyzed by phenylalanine ammonia-lyase. *Plant Cell 16*, 3426–3436.

(18) Montavon, T. J., Christianson, C. V., Festin, G. M., Shen, B., and Bruner, S. D. (2008) Design and characterization of mechanism-based inhibitors for the tyrosine aminomutase SgTAM. *Bioorg. Med. Chem. Lett. 18*, 3099–3102.

(19) Arnold, K., Bordoli, L., Kopp, J., and Schwede, T. (2006) The SWISS-MODEL workspace: a web-based environment for protein structure homology modelling. *Bioinformatics 22*, 195–201.

(20) Bailey, S. (1994) The CCP4 suite: programs for protein crystallography. *Acta Crystallogr., Sect. D D50*, 760–763.

(21) Emsley, P., Lohkamp, B., Scott, W. G., and Cowtan, K. (2010) Features and development of Coot. *Acta Crystallogr., Sect. D 66*, 486–501.

(22) Mutatu, W., Klettke, K. L., Foster, C., and Walker, K. D. (2007) Unusual mechanism for an aminomutase rearrangement: retention of configuration at the migration termini. *Biochemistry 46*, 9785–9794.

(23) Calabrese, J. C., Jordan, D. B., Boodhoo, A., Sariaslani, S., and Vannelli, T. (2004) Crystal structure of phenylalanine ammonia lyase: Multiple helix dipoles implicated in catalysis. *Biochemistry 43*, 11403–11416.

(24) Moffitt, M. C., Louie, G. V., Bowman, M. E., Pence, J., Noel, J. P., and Moore, B. S. (2007) Discovery of two cyanobacterial phenylalanine ammonia lyases: Kinetic and structural characterization. *Biochemistry 46*, 1004–1012.

(25) Louie, G. V., Bowman, M. E., Moffitt, M. C., Baiga, T. J., Moore, B. S., and Noel, J. P. (2006) Structural determinants and modulation of substrate specificity in phenylalanine-tyrosine ammonia-lyases. *Chem. Biol. 13*, 1327–1338.

(26) Schwede, T. F., Rétey, J., and Schulz, G. E. (1999) Crystal structure of histidine ammonia-lyase revealing a novel polypeptide modification as the catalytic electrophile. *Biochemistry 38*, 5355–5361.

(27) Szymanski, W., Wu, B., Weiner, B., de Wildeman, S., Feringa, B. L., and Janssen, D. B. (2009) Phenylalanine aminomutase-catalyzed addition of ammonia to substituted cinnamic acids: A route to enantiopure α- and β-amino acids. *J. Org. Chem. 74*, 9152–9157.

(28) Röther, D., Poppe, L., Morlock, G., Viergutz, S., and Rétey, J. (2002) An active site homology model of phenylalanine ammonia-lyase from *Petroselinum crispum. Eur. J. Biochem. 269*, 3065–3075.

(29) Röther, D., Poppe, L., Viergutz, S., Langer, B., and Rétey, J. (2001) Characterization of the active site of histidine ammonia-lyase from *Pseudomonas putida. Eur. J. Biochem. 268*, 6011–6019.

(30) Poppe, L., Pilbak, S., Paizs, C., and Retey, J. (2008) Mechanistic aspects and biocatalytic implications of the MIO-containing ammonia-lyase/aminomutase family. *Stud. Univ. Babes-Bolyai, Chem. 53*, 15–19.

(31) Sawada, S., Kumagai, H., Yamada, H., Hill, R. K., Mugibayashi, Y., and Ogata, K. (1973) Stereochemistry of ammonia elimination from L-tyrosine with L-phenylalanine ammonia-lyase. *Biochim. Biophys. Acta 315*, 204–207.

(32) Ellis, B. E., Zenk, M. H., Kirby, G. W., Michael, J., and Floss, H. G. (1973) Steric course of the tyrosine ammonia-lyase reaction. *Phytochemistry 12*, 1057–1058.

(33) Hanson, K. R., and Havir, E. A. (1970) L-Phenylalanine ammonia-lyase: IV. Evidence that the prosthetic group contains a dehydroalanyl residue and mechanism of action. *Arch. Biochem. Biophys.* 141, 1–17.

(34) Jennewein, S., Wildung, M. R., Chau, M., Walker, K., and Croteau, R. (2004) Random sequencing of an induced *Taxus* cell cDNA library for identification of clones involved in Taxol biosynthesis. *Proc. Natl. Acad. Sci. U.S.A. 101*, 9149–9154.